# Supplementary information for
# Giant converse magnetoelectric effect in a multiferroic heterostructure with polycrystalline $Co_2FeSi$

Shumpei Fujii,[†] Takamasa Usami,[‡] Yu Shiratsuchi,[¶,‡] Adam M. Kerrigan,[§] Amran Mahfudh Yatmeidhy,[‖] Shinya Yamada,[‡,†] Takeshi Kanashima,[†] Ryoichi Nakatani,[¶,‡] Vlado K. Lazarov,[§] Tamio Oguchi,[‡] Yoshihiro Gohda,[‖,‡] and Kohei Hamaya[*,‡,†]

†*Department of Systems Innovation, Graduate School of Engineering Science, Osaka University, 1-3 Machikaneyama, Toyonaka, Osaka 560-8531, Japan.*

‡*Center for Spintronics Research Network, Graduate School of Engineering Science, Osaka University, 1-3 Machikaneyama, Toyonaka, Osaka 560-8531, Japan.*

¶*Division of Materials and Manufacturing Science, Graduate School of Engineering, Osaka University, Suita, Osaka 565-0871, Japan.*

§*Department of Physics, University of York, York YO10 5DD, United Kingdom.*

‖*Department of Materials Science and Engineering, Tokyo Institute of Technology, J1-3, Nagatsuta-cho 4259, Midori-ku, Yokohama 226-8502, Japan*

E-mail: hamaya.kohei.es@osaka-u.ac.jp

## S1 & 2: Nanobeam diffraction of $Co_2FeSi$ grains and PMN-PT(001)

Supplementary Figures S1 and S2 display the nanodiffraction analysis of the $Co_2FeSi$ film on PMN-PT(001) substrate. By using the [011] orientation of PMN-PT as a reference (Fig. S1**b**), we present $Co_2FeSi$ grains within the film that are oriented along [422] orientation (Fig. S1**d**), and along [220] direction (Fig. S2**d**). As a reference we also present calculated diffraction patterns of the substrate along [001] and $[11\bar{1}]$ in Fig.S1**c** and Fig.S2**c**, respectively. Similarly the calculated diffraction patterns from $L2_1$-ordered phase of $Co_2FeSi$, along [110] direction and [001] direction are presented in Fig. S1**e** and Fig. S2**e**, respectively. Finally we note that Fig. S1**d** also shows the [111] type of reflections, which is the signature of $L2_1$-ordering.

## S3: XRD measurements for $Co_2FeSi$/Fe/PMN-PT(011) heterostructures

Figure S3**a** displays an x-ray diffraction (XRD) $\omega$-$2\theta$ scan (out-of-plane) profile for a $Co_2FeSi$/PMN-PT(011) heterostructure. To identify the XRD patterns, we have measured the XRD profiles only for the PMN-PT substrate and only for the sample holder, in addition to $Co_2FeSi$/Fe/PMN-PT(011) heterostructures. Very weak diffraction peaks from the (220) and (422) planes for $Co_2FeSi$ are observed at around $2\theta = 45.5$ and 84.1 degrees, respectively. Thus, the grown $Co_2FeSi$ film is not highly oriented structure on PMN-PT(011) and is polycrystalline. In Fig. S3**b** the pole figure measured at $2\theta = 45.0$ degree indicates the presence of $\{202\}$ or $\{220\}$ diffraction peaks, meaning the presence of the basic reflection of the cubic crystal structure. Because we also showed the presence of $\{111\}$ diffraction peaks in the main manuscript (Fig. 1**e**), we can judge that the $L2_1$-ordered structure is included in the polycrystalline $Co_2FeSi$ film.

## S4: Polarization switching process of PMN-PT(011).

When an electric field ($E$) is applied to the [110] direction of the PMN-PT(011) substrate, the polarization switching process can be explained generally, given in the relevant literature.[1–3] Figure S4**a** is the same as Fig. 2**a** in the main manuscript and shows the unpoled state of PMN-PT(011). Since the spontaneous piezoelectric polarizations lie along the diagonals of the (011) plane and ($01\bar{1}$) plane, there is no lattice deformation in the (011) plane, as shown in the bottom of **a**. When a negative value of $E$ such as $-$ 0.8 MV/m is applied to the [011] direction of the PMN-PT(011) substrate, all of the eight possible polarization vectors are switched toward the directions shown in Fig. S4**b**. As a consequence, the lattice deformation in the (011) plane is induced, as shown in the bottom of **b**. By switching the direction of $E$ and increasing $E$ (Fig. S4**c**), on the other hand, the polarization vectors are restored, leading to the elongation of the lattice constant along the PMN-PT[100] direction (the bottom of **c**). Thus, it is generally known that the direction of the lattice deformation in the (011) plane along the PMN-PT[100] direction is changed from the contraction to the elongation before the switching of the polarization vectors. When the applied $E$ is switched from negative to positive, the polarization vectors of the PMN-PT(011) are switched, as shown in Figs. S4**d** and **e**. As a result, the lattice deformation in the (011) plane along the PMN-PT[100] direction can be changed again from the elongation to the contraction. Therefore, the anisotropic piezostrains of the PMN-PT(011) substrate can be utilized to induce the variation in an in-plane uniaxial magnetic anisotropy for ferromagnetic materials.[1–3]

## S5: Reproducibility of the giant CME effect.

To confirm the reliability of the observed CME effect in Fig. 3**a**, we also measure other $Co_2FeSi$/PMN-PT(011) heterostructures. Figures S5**a** and **b** show the magnitude of the magneto-optic Kerr ellipticity ($\eta_R$) and $\alpha_E$ as a function of $E$, respectively, for another representative $Co_2FeSi$/PMN-PT(011) heterostructure in the measurement along the PMN-PT[100] direction at room temperature. As seen in Fig. S5**a**, the hysteretic nature is reproducibly observed and there are two stable states at $E = 0$. We also obtain the giant $\alpha_E$ of more than $1.0 \times 10^{-5}$ s/m at $E \sim -$ 0.25 MV/m and 0. Thus, the nonvolatile feature at around $E = 0$ and the giant CME effect are reproduced in other $Co_2FeSi$/PMN-PT(011) heterostructures although slight differences are included between samples.

## S6: Anisotropic piezoelectric response in the PMN-PT(011).

To consider the piezoelectric effect of the $Co_2FeSi$/PMN-PT(011) heterostructures, we also measured the values of strain $\varepsilon$ (ppm) as a function of $E$ for the PMN-PT(011) substrate at room temperature. Figures S6**a** and **b** show the in-plane strain curves for the PMN-PT(011) measured along the PMN-PT[100] and PMN-PT[$01\bar{1}$] directions, respectively. A hysteretic butterfly shape is seen in the $\varepsilon_{[100]} - E$ curve (**a**), indicating simple features that can be understood in Fig. S4. Here the asymmetric shape with respect to $E = 0$ is due to the unintentionally induced difference in the quality of the top and bottom contacts. On the other hand, the shape of the $\varepsilon_{[01\bar{1}]} - E$ curve (**b**) is evidently different from the butterfly shape. In addition, the bistable behavior at $E = 0$, almost the same feature discussed in a previous work.[3] To observe the anisotropic strain, we extract the plot of $(\varepsilon_{[01\bar{1}]} - \varepsilon_{[100]})$ as a function of $E$, as shown in Fig. S6**c**. As a result, we can also see the two states at $E = 0$, as previously shown by Wang *et al.*[3]

## S7: Characterization of a $Fe_3Si$/PMN-PT(011) heterostructure.

For comparison, we formed $Fe_3Si$/PMN-PT(011) heterostructures, where the $Fe_3Si$ layer was grown by MBE.[4] During the growth of $Fe_3Si$, we can observe the marked difference in the RHEED patterns between the PMN-PT[$01\bar{1}$] and PMN-PT[100] azimuths in Fig. S7**a**. This feature is almost the same as that for $Co_2FeSi$, as shown in Fig. 1**c**. From XRD measurements, we can obtain almost the same features as those for $Co_2FeSi$. Since the $\omega$-$2\theta$ scan (out-of-plane) indicated the weak diffraction peaks from the (220) and (422) planes, the grown $Fe_3Si$ layer is polycrystalline. In addition, the pole figures in Fig. S7**b** clearly show the presence of $D0_3$-ordered structures in the polycrystalline $Fe_3Si$ layer on PMN-PT(011). Therefore, the crystal quality of the $Fe_3Si$ layer on PMN-PT(011) is nearly equal to that of the $Co_2FeSi$ layer on PMN-PT(011).

In Fig. S7**c** we present magnetic-field ($H$)-dependent magnetization at room temperature, measured along the PMN-PT[$01\bar{1}$] and PMN-PT[100] crystallographic directions in the film plane. Like a $Co_2FeSi$/PMN-PT(011) heterostructure, we can also observe an anisotropic feature of the magnetization curves along the two different crystal axes for the $Fe_3Si$/PMN-PT(011) heterostructure. However, the induced uniaxial anisotropy is slightly small (4.9 kJ/$m^3$) compared to that in $Co_2FeSi$ (5.8 kJ/$m^3$). Notably, the value of $M_S$ (940 ± 10 kA/m) is nearly the same one in our previous work on epitaxial $Fe_3Si$ films.[4]

# References


1. Zhang, S., Zhao, Y., Xiao, X., Wu, Y., Rizwan, S., Yang, L., Li, P., Wang, J., Zhu, M., Zhang, H., Jin, X., & Han, X., Giant electrical modulation of magnetization in $Co_{40}Fe_{40}B_{20}/Pb(Mg_{1/3}Nb_{2/3})_{0.7}Ti_{0.3}O_3$(011) heterostructure, *Sci. Rep.* **4**, 3727 (2014).

2. Liu, M., Nan, T., Hu, J.- M., Zhao, S. S., Zhou, Z., Wang, C. Y., Jiang, Z. D., Ren, W., Ye, Z. G., Chen, L. Q. & Sun, N. X. Electrically controlled non-volatile switching of magnetism in multiferroic heterostructures via engineered ferroelastic domain states. *NPG Asia Mater.* **8**, e316 (2016).

3. Wang, J., Pesquera, D., Mansell, R., Van Dijken, S., Cowburn, R. P., Ghidini, M. & Mathur, N. D. Giant non-volatile magnetoelectric effects via growth anisotropy in $Co_{40}Fe_{40}B_{20}$ films on PMN-PT substrates. *Appl. Phys. Lett.* **114**, 092401 (2019).

4. Yamada, S., Sagar, J., Honda, S., Lari, L., Takemoto, G., Itoh, H., Hirohata, A., Mibu, K., Miyao, M., & Hamaya, K. Room-temperature structural ordering of a Heusler compound $Fe_3Si$. *Phys. Rev. B* **86**, 174406 (2012).

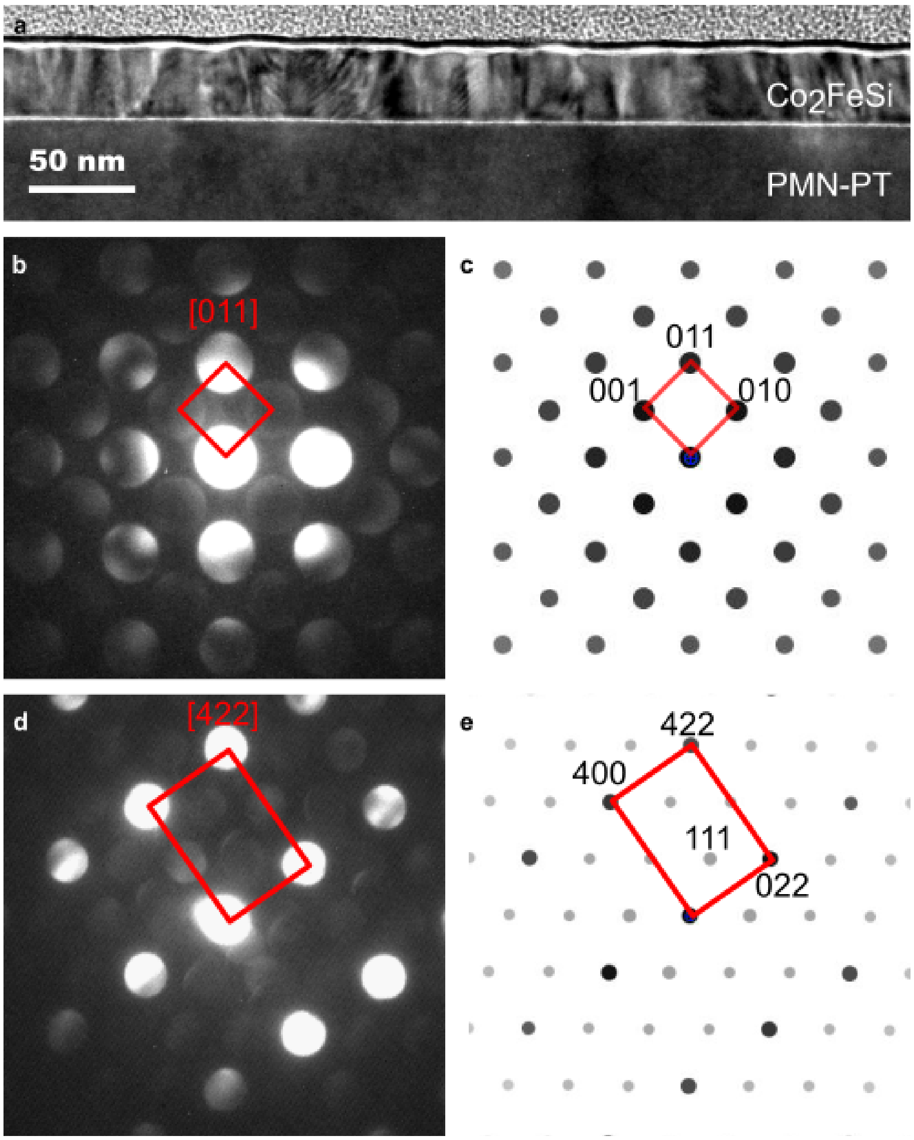


Figure S 1: **a.** BF-TEM image of textured $Co_2FeSi$ film grown on PMN-PT(011) substrate. **b.** Nanobeam diffraction of the substrate confirming the substrate is (011) terminated. **c.** Simulated diffraction pattern for the [100] zone axis in PMN-PT confirming the orientations shown in **b**. **d.** Nanobeam diffraction of a single grain within the textured $Co_2FeSi$ film showing $L2_1$-ordering and (422) termination. **e.** Simulated diffraction pattern for the $[01\bar{1}]$ zone axis in $Co_2FeSi$ confirming the orientations shown in **d**.

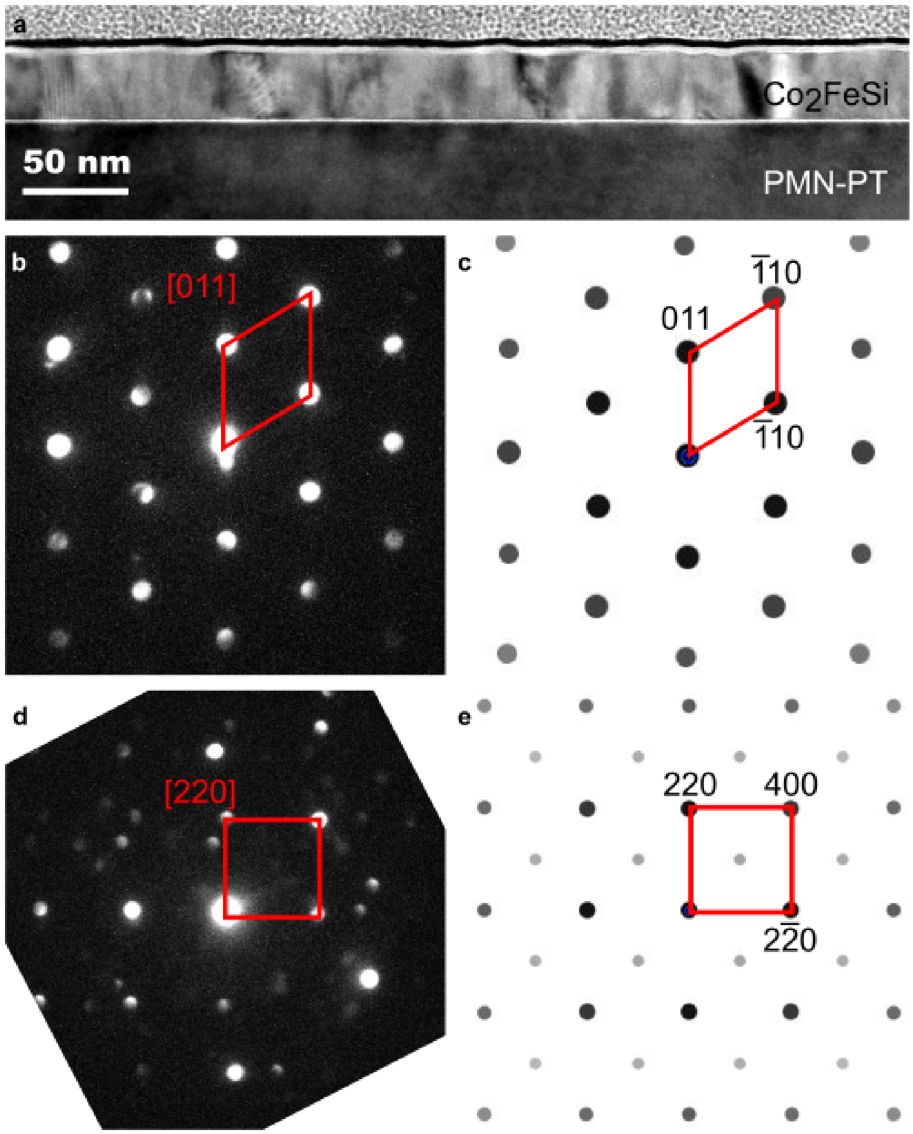


Figure S 2: **a.** BF-TEM image of textured $Co_2FeSi$ film grown on PMN-PT(011) substrate. **b.** Nanobeam diffraction of the substrate confirming the substrate is (011) terminated. **c.** Simulated diffraction pattern for the $[11\bar{1}]$ zone axis in PMN-PT confirming the orientations shown in **b**. **d.** Nanobeam diffraction of two overlapping grains within the textured $Co_2FeSi$ film with the (220) terminated grain highlighted. **e.** Simulated diffraction pattern for the [001] zone axis in $Co_2FeSi$ confirming the orientations shown in **d**.

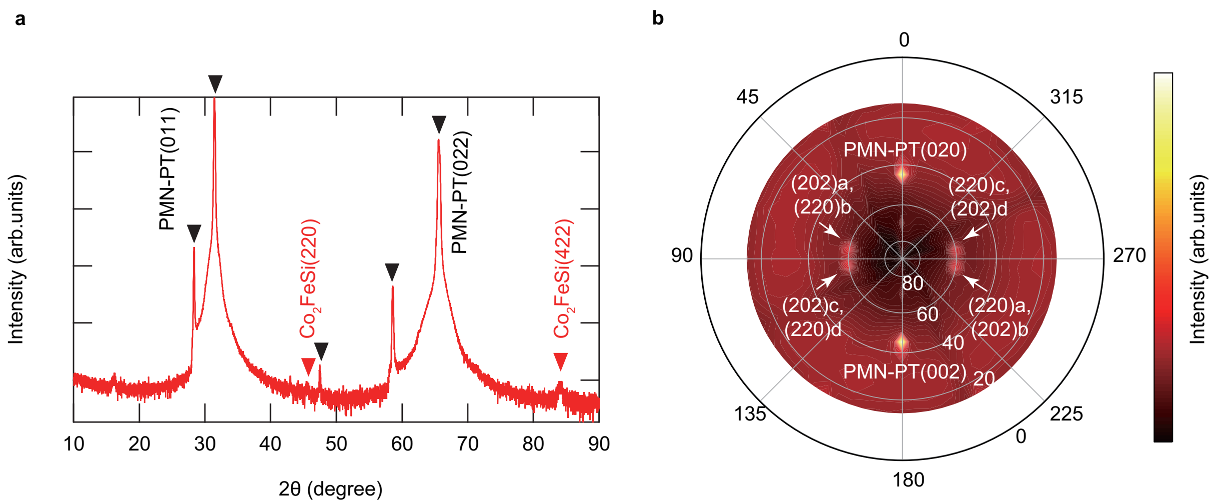


Figure S 3: **a.** XRD $\omega$-$2\theta$ profile (out-of-plane) of a $Co_2FeSi$/PMN-PT(011) heterostructure. **b.** XRD pole figure (in-plane) of $Co_2FeSi$ on PMN-PT(011), measured at $2\theta = 45.0$ degree.

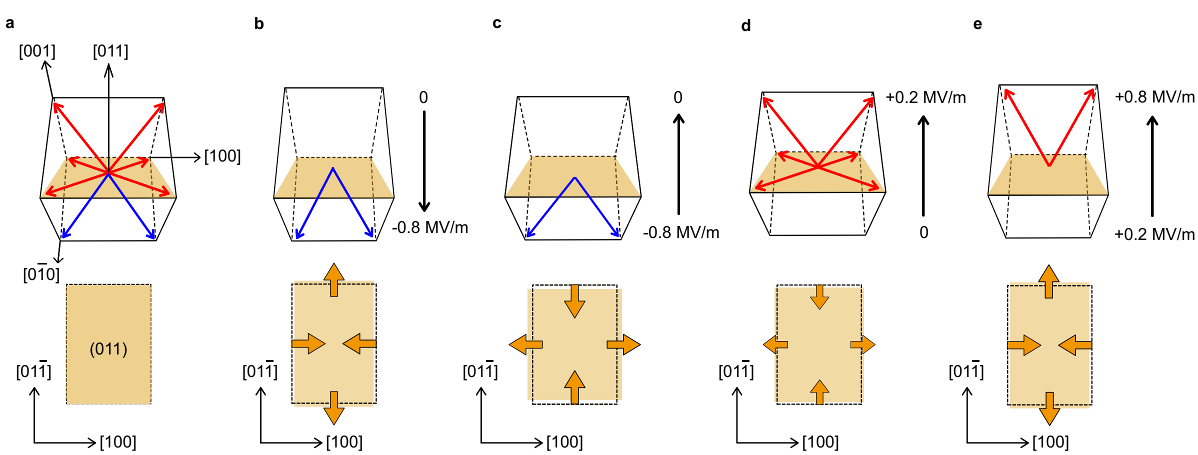


Figure S 4: **a.** Schematic of the correlation between polarization vectors and crystal orientations of (011)-oriented PMN-PT substrate in the unpoled state. **b - e.** When the external $E$ is applied along the PMN-PT[011] direction, the polarization vectors (top) and lattice deformation of the (011) plane (bottom) are varied.

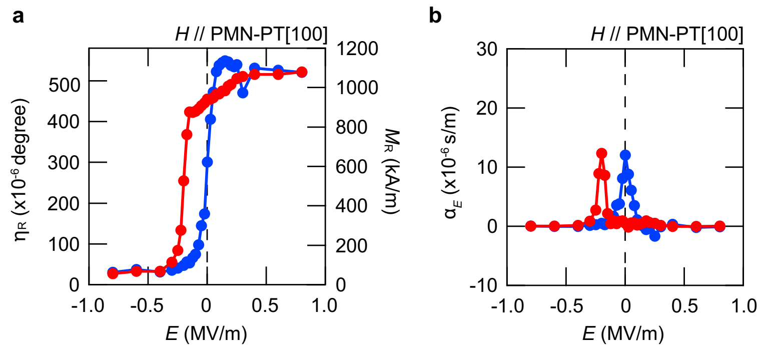


Figure S 5: $E$-dependent $\eta_{\mathrm{R}}$ (**a**) and $\alpha_{\mathrm{E}}$ (**b**), measured along PMN-PT[100] at room temperature, for another $Co_2FeSi$/PMN-PT(011) heterostructure. The blue or red curve is measured after the $E$ sweeping from $-$ 0.8 MV/m to 0 or from + 0.8 MV/m to 0, respectively.

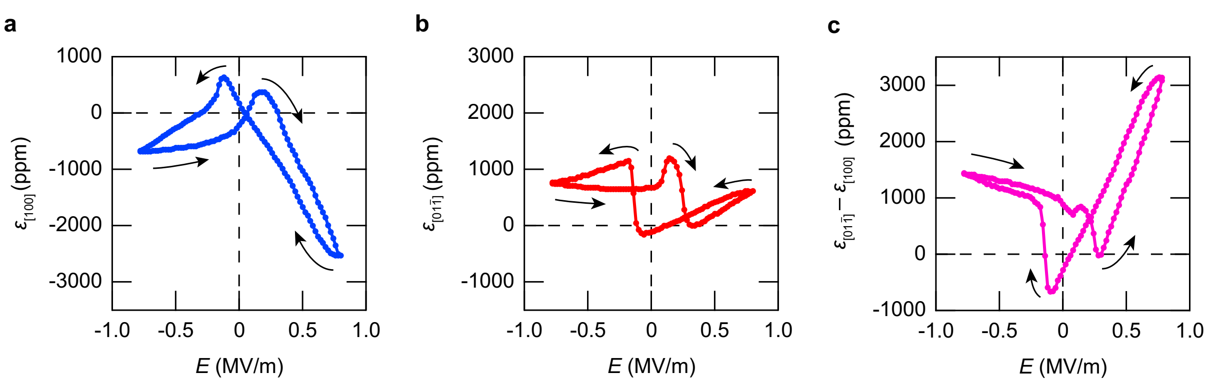


Figure S 6: In-plane piezoelectric curves measured along [100] (**a**) and $[01\bar{1}]$ (**b**) for the PMN-PT(011) substrate the at room temperature. **c.** Anisotropy of the in-plane strain ($\varepsilon_{[01\bar{1}]} - \varepsilon_{[100]}$) as a function of $E$.

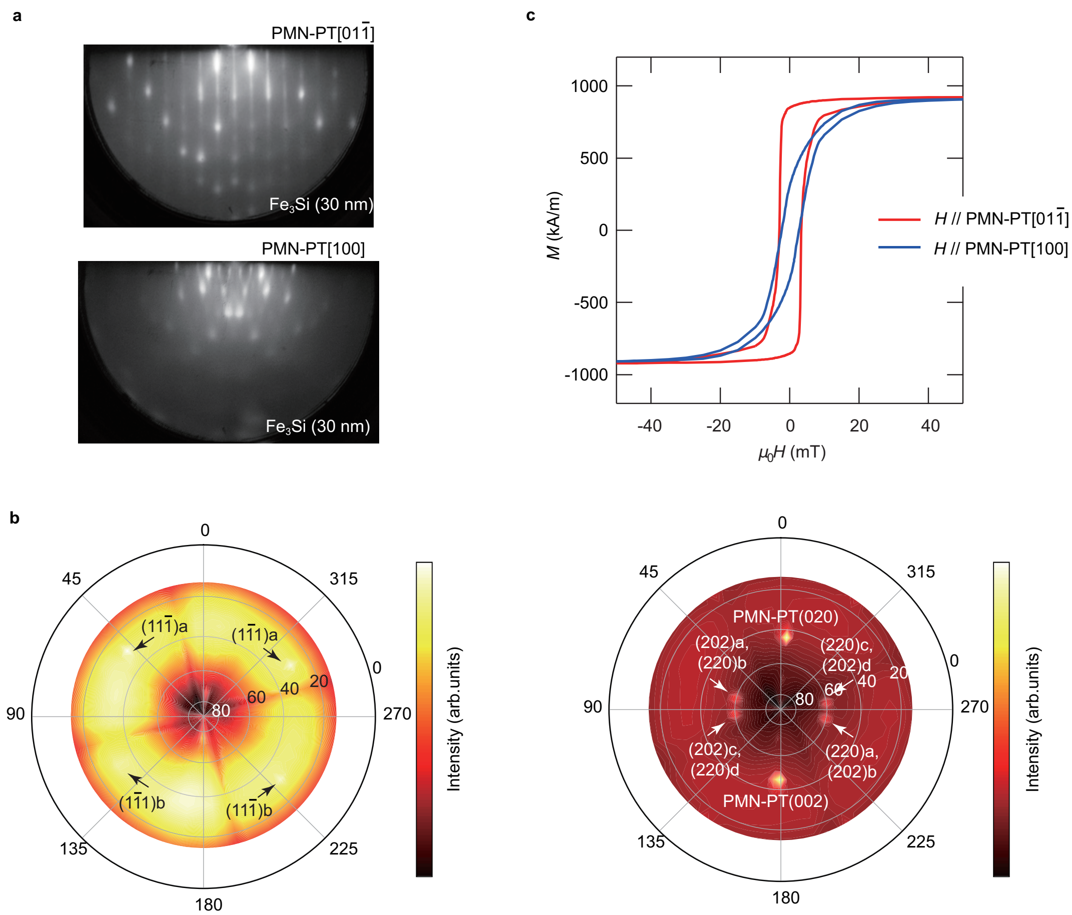


Figure S 7: **a.** RHEED patterns for the $Fe_3Si$ layer during the growth along the PMN-PT[01$\bar{1}$] and PMN-PT[100] directions under the observations. **b.** XRD pole figures for the presence of $D0_3$-ordered structures in $Fe_3Si$ on PMN-PT(011). **c.** Magnetization hysteresis curves at 300 K under $H$ along the PMN-PT[01$\bar{1}$] (red) and PMN-PT[100] (blue) directions.